JOURNAL OF THE AMERICAN CHEMICAL SOCIETY

Communication

pubs.acs.org/JACS

# $[Pd_4(\mu_3\text{-}SbMe_3)_4(SbMe_3)_4]$: A Pd(0) Tetrahedron with $\mu_3$-Bridging Trimethylantimony Ligands

Sophie L. Benjamin,[*,†] Tobias Krämer,[*,‡] William Levason,[§] Mark E. Light,[§] Stuart A. Macgregor,[‡] and Gillian Reid[§]

[†]School of Science and Technology, Nottingham Trent University, Nottingham NG11 8NS, United Kingdom

[‡]Institute of Chemical Sciences, Heriot-Watt University, Edinburgh EH14 4AS, United Kingdom

[§]School of Chemistry, University of Southampton, Southampton SO17 1BJ, United Kingdom

Supporting Information

**ABSTRACT:** The palladium(II) chlorostibine complex $[PdCl_2(SbMe_2Cl)_2]_2$ has a dimeric structure in the solid state, stabilized by hyper-coordination at the Lewis amphoteric Sb centers. Reaction with 8 equiv of MeLi forms $[Pd_4(\mu_3\text{-}SbMe_3)_4(SbMe_3)_4]$, whose structure comprises a tetrahedral Pd(0) core with four terminal $SbMe_3$ ligands and four $\mu_3$-$SbMe_3$ ligands, one capping each triangular $Pd_3$ face. Density functional theory calculations, supported by energy decomposition analysis and the natural orbitals for chemical valence scheme, highlight significant donor and acceptor orbital contributions to the bonding between both the terminal and the bridging $SbMe_3$ ligands and the $Pd_4$ core.

Despite their ubiquity in modern coordination chemistry, it was long thought that phosphine ligands and their heavier pnictine congeners ($PnR_3$; Pn = P, As, Sb, Bi) were terminal donors only, while other $\pi$-acceptor ligands such as CO are frequently found to bridge more than one metal center. Werner was the first to challenge this concept, with the isolation of a $Rh_2$ dimer bridged by $Sb^iPr_3$ (Figure 1, i), its

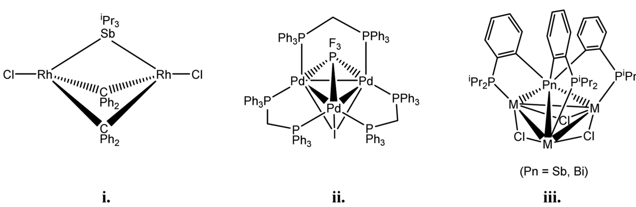


**Figure 1.** Complexes with bridging pnictine ligands (refs 1−5).

subsequent ligand metathesis giving rise to the first examples of $\mu_2$-bridging $PR_3$ and $AsR_3$.[1,2] Despite this breakthrough, very few other systems with bridging pnictines have since been characterized; Balch isolated a few examples of $PF_3$ triply bridging a $Pd_3$ triangle (Figure 1, ii),[3,4] and Gabbaï recently reported the complexation of a tetradentate $P_3Pn$ ligand (Pn = Sb, Bi) with a $M_3$ triangle (M = Cu, Ag) in which the heavy pnictine donor is supported centrally above the $M_3$ face (Figure 1, iii).[5] Because of the rarity of such species, little is known about the nature of the bonding in these complexes. Based on the limited examples, the bridging mode seems to feature a significant component of acceptance by the ligand and is best stabilized by late transition metals in low oxidation states and strongly $\pi$-accepting or heavier, more Lewis acidic pnictines.[6]

There has been a surge of recent interest in the "non-innocent" behavior of coordinated heavy pnictines, which in several cases demonstrate redox reactivity or anion exchange at Pn in preference to the transition metal center.[7,8] They are also prone to hyper-coordination, forming intra- or intermolecular secondary acceptor interactions with electronegative donor atoms; this behavior is enhanced by electronegative substituents on the pnictine, which increase the Lewis acidity of the Pn center.[9] We have previously demonstrated that increasing the number of halide substituents in $SbBr_nMe_{3-n}$ ($n$ = 0−2) increases the $\pi$-acceptor capacity of the stibine ligand.[10] While triorganopnictines are $\sigma$-donor/$\pi$-acceptor ligands, halide-substituted Sb and Bi centers have been seen to act as $\sigma$-acceptors toward electron-rich transition metals, giving rise to complexes with highly unusual electronic strutures.[11−14]

We report here an unusual dimeric Pd(II) complex of $SbMe_2Cl$ which demonstrates significant Lewis acidity of the bound halostibine. The reaction of this complex with MeLi leads to formation of an unexpected Pd(0) cluster featuring both terminal and triply bridging $SbMe_3$ ligands; the first example of an unsupported $\mu_3$-organopnictine ligand.

The reaction of $[PdCl_2(MeCN)_2]$ with 2 equiv of $SbMe_2Cl$ resulted in the formation of $[PdCl_2(SbMe_2Cl)_2]$ as a red solid in good yield, which appears stable in air for several hours (Scheme 1). The expected singlet was observed in the $^1H$ NMR spectrum as well as a single broad $^{13}C\{^1H\}$ NMR resonance. The solid-state far IR spectrum shows two bands corresponding to Pd−Cl stretches ($C_{2v}$: $A_1 + B_1$). Crystals were grown from the benzene filtrate and analyzed by X-ray crystallography. The solid-state structure comprises the centrosymmetric dimeric unit $[PdCl_2(SbMe_2Cl)_2]_2$, consisting of two distorted square planar Pd centers with *cis* chloride and chlorostibine ligands, connected by a fairly short Pd(II)−Pd(II) interaction (2.9143(4) Å) (Figure 2).

Most examples of Pd(II) dimers feature bidentate bridging ligands supporting the Pd−Pd interaction. One rare counter-example is the diaminosugar complex $[Pd(C_7H_{16}N_2O_2)Cl_2]_2$ (Pd−Pd = 3.284 Å), in which dimerization is supported by H-

**Received:** April 20, 2016

  

**Scheme 1. Synthesis of $[PdCl_2(SbMe_2Cl)_2]_2$ and $[Pd_4(\mu_3\text{-}SbMe_3)_4(SbMe_3)_4]$**

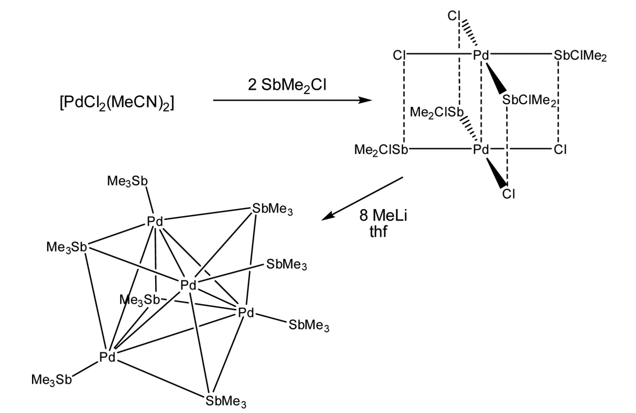


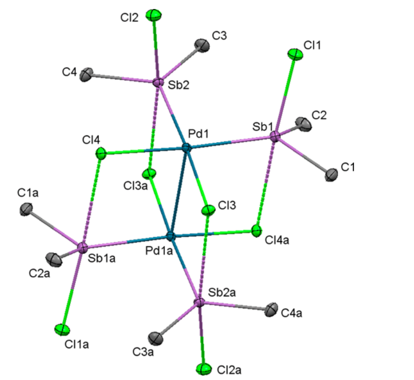


**Figure 2.** View of the structure of $[PdCl_2(SbMe_2Cl)_2]_2$. Ellipsoids are drawn at 50% probability levels and H atoms are omitted for clarity. Secondary Sb···Cl interactions are indicated by dashed bonds. Symmetry operation $a = 2 - x, 1 - y, 1 - z$.

bonding between amine and Cl ligands.[15] A similar conformation is adopted by $[PdCl_2(SbMe_2Cl)_2]_2$; each chlorostibine ligand eclipses a Cl ligand on the opposite Pd center when viewed down the Pd–Pd vector (torsion angles: Cl4–Pd1–Pd1a–Sb1a = 3.94(3)° Cl3–Pd1–Pd1a–Sb2a = 5.68(3)°), leading to very short intermolecular Sb–Cl distances (mean 2.96 Å, cf. mean Sb–Cl covalent = 2.39 Å, $\Sigma_{vdW}$ = 4.29 Å).[16]

The propensity of coordinated Sb or Bi donors to act simultaneously as acceptors, forming intra- or intermolecular "hypervalent" interactions with electronegative atoms, is a current area of interest,[8,9] and it has been demonstrated that these interactions can strongly direct the solid-state structure of a complex.[17] It appears that in $[PdCl_2(SbMe_2Cl)_2]_2$, four such Sb···Cl interactions support the formation of the dimeric species. These interactions form approximately *trans* to the covalently bonded halide substituent on Sb (mean ∠ Cl···Sb–Cl = 169.0°), the Sb–Cl $\sigma^*$ being the most accessible acceptor orbital on Sb. Consistent with this, natural bond orbital (NBO) analysis identifies a notable $3p_{Cl} \rightarrow \sigma^*_{Sb-Cl}$ interaction (see SI for further details). The geometry at Sb is near trigonal bipyramidal, severely distorted from the expected pseudotetrahedral. The structure is reminiscent of that of the Pt(II)–Pt(II) dimer $[PtCl_2\{CH_2(o\text{-}C_6H_4CH_2SbMe_2)\}_2]_2$, which contains weak intermolecular Sb···Cl contacts (mean 3.48 Å);[18] the considerably shorter Sb···Cl distances found in $[PdCl_2(SbMe_2Cl)_2]_2$ can be accounted for by the increased acceptor power of the halostibine in comparison to the triorganostibine. In each case it is difficult to separate the magnitude of the secondary Sb···Cl interaction from that of the metallophilic interaction between the group 10 metals.

There are very few previous reports of halostibine complexes with transition metal halides. In view of the recent interest surrounding the "noninnocent" behavior of coordinated stibines, we investigated the reactivity of $[PdCl_2(SbMe_2Cl)_2]_2$ with reagents which specifically have the potential to target both the Pd and Sb metal centers. Treatment of $[PdCl_2(SbMe_2Cl)_2]_2$ with 8 equiv of MeLi (equimolar with Cl) in tetrahydrofuran resulted in the formation of an intensely violet solution, from which a dark purple solid was isolated (Scheme 1). The product is stable over several weeks when stored under an $N_2$ atmosphere, but slowly becomes black/brown in contact with air. It is remarkably soluble in *n*-hexane and less soluble in chlorinated solvents. Small purple crystals were analyzed by X-ray diffraction, giving the solid-state structure shown in Figure 3, formulated as $[Pd_4(\mu_3\text{-}SbMe_3)_4(SbMe_3)_4]$.

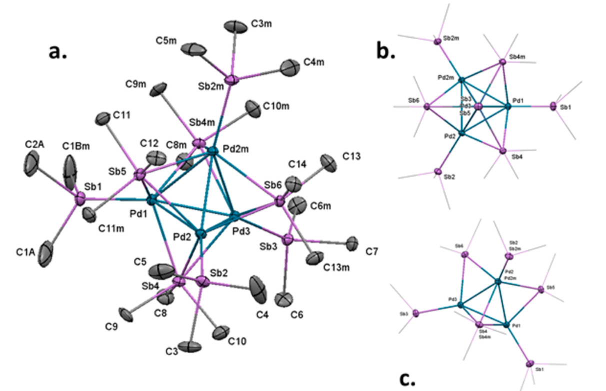


**Figure 3.** Views of the structure of $[Pd_4(\mu_3\text{-}SbMe_3)_4(SbMe_3)_4]$. Ellipsoids are drawn at 50% probability, and H atoms are omitted for clarity. Only one of two symmetry equivalent positions shown for the Me substituents of Sb1. Symmetry operation $m = 1 - x, + y, + z$. (a) Best view; (b) down a $Sb_{terminal}$–Pd···$Sb_{bridging}$ vector; (c) down the *a*-axis. C atoms are drawn as wireframe in (b) and (c).

The structure comprises a central tetrahedron of four Pd(0) atoms, with an average Pd–Pd distance of 2.805 Å. Each Pd is coordinated to one terminal $SbMe_3$ ligand (mean Pd–Sb = 2.520 Å) and one $SbMe_3$ ligand caps each face of the tetrahedron, bridging three Pd atoms (mean Pd–Sb = 2.773 Å). A mirror plane bisects the tetrahedron, passing through two Pd atoms, two bridging Sb, and two terminal Sb atoms. There is symmetry-related disorder of the Me substituents on the terminal Sb1. Each bridging $SbMe_3$ ligand is almost equidistant from the three Pd atoms it caps; the least symmetrical is Sb5, with a difference of 0.07 Å between Sb5–Pd1 and Sb5–Pd2. The most symmetrical, Sb4, has <0.01 Å difference between Sb4–Pd1, Sb4–Pd2, and Sb4–Pd3. The molecule has near $C_{3v}$ symmetry, but attempts to solve the diffraction data in higher symmetry space groups were unsatisfactory; the $Cmc2_1$ solution is correct. Figure 3b,c shows alternative views of the structure in which this pseudosymmetry can be clearly discerned.

The $^1H$ and $^{13}C\{^1H\}$ NMR spectra of $[Pd_4(\mu_3\text{-}SbMe_3)_4(SbMe_3)_4]$ in benzene-$d_6$ solution each display two broad resonances of equal intensity, corresponding to two


DOI: 10.1021/jacs.6b04060
J. Am. Chem. Soc. XXXX, XXX, XXX–XXX

distinct $SbMe_3$ environments. This is consistent with the conservation of the tetramer in solution, the broadening of the peaks being most likely due to the proximity of the quadrupolar Sb nuclei ($^{121}$Sb $I = 5/2$; $^{123}$Sb $I = 7/2$). The identity of the product is supported by elemental analysis.

The triply bridging behavior of a monodentate organopnictine ligand is unprecedented. Of the two systems previously reported which feature $\mu_3$-pnictines, the first involves $PF_3$, a strong $\pi$-acceptor ligand which can be considered as electronically more akin to CO than to $PR_3$. In $[Pd_3(\mu_3\text{-}PF_3)(\mu\text{-}X)(\mu\text{-}dppm)_3]^+$ (X = Cl, I; dppm = bis(diphenylphosphino)methane), the $PF_3$ unit bridges an equilateral triangle of Pd(0)/(I) atoms (Figure 1, ii), which bears a significant resemblance to the faces of the Pd(0) tetrahedron discussed here; the Pd−Pd distances are somewhat shorter (2.58−2.60 Å).[3,4] The second (Figure 1, iii), $[M_3(\mu\text{-}Cl)_3(o\text{-}\{^iPr_2P\}\text{-}C_6H_4)_3Pn]$ (M = Cu, Ag; Pn = Sb, Bi) features a tetradentate ligand in which M−P bonding constrains the heavy pnictogen atom in a bridging position over the center of the $M_3$ triangle.[5] NBO calculations demonstrated significant Pn → M donor interactions as well as weaker Pn ← M acceptor interactions, amounting to a symmetrical four-center two-electron bridging $PnM_3$ interaction.

The structure of $[Pd_4(\mu_3\text{-}SbMe_3)_4(SbMe_3)_4]$ is particularly unexpected given that the bridging $SbMe_3$ is unsupported, i.e., not stabilized by polydentate bridging moieties, and that $SbMe_3$ might be expected to be only a moderate $\pi$-acceptor. The cluster is held together entirely by $\mu_3$-$SbMe_3$ bridges and Pd−Pd interactions. Comparable $Pd(0)_4$ clusters with terminal phosphines and $\mu_2$-bridging CO or $SO_2$ ligands have been reported with similar Pd−Pd distances, though they are generally of lower symmetry.[19,20] Recently, the unusual $[\{Pd(CN^tBu)\}_4(GaCp^*)_4]$ cluster was reported, containing a highly symmetric $Pd_4Ga_4$ core, comparable to the $Pd_4Sb_4$ core of $[Pd_4(\mu_3\text{-}SbMe_3)_4(SbMe_3)_4]$, with a similar Pd−Pd distance (2.875 Å) and Pd−Ga distances of 2.535 Å.[21]

Density functional theory (DFT) was employed to provide insight into the electronic structure of $[Pd_4(\mu_3\text{-}SbMe_3)_4(SbMe_3)_4]$. Full geometry optimization under $C_1$ symmetry afforded a structure with bond parameters closely matching the crystal structure. However, to facilitate the analysis, we used a $C_{3v}$-optimized geometry: this lies only 3 kcal mol$^{-1}$ above the $C_1$ minimum and leaves the approximately tetrahedral geometry essentially unchanged (Table S1 and Figure S1).

The formal cluster electron count of 56 for $[Pd_4(\mu_3\text{-}SbMe_3)_4(SbMe_3)_4]$ is 4 electrons fewer than the predicted valence electron count of 60 for a tetrahedron with localized bonding. Such an ideal count is exemplified in $[Ni_4(CO)_6(P(C_2H_4CN)_3)_4]$ ($T_d$ symmetry),[22] which contains 6 edge-bridging carbonyls and 4 terminal phosphine ligands at the vertices. However, stable electron-deficient clusters are not uncommon for the heavier group 10 metals,[20,23−26] which often form stable compounds that do not conform to the 18-electron rule, a fact attributed to the increased energy gap between the valence d and p orbitals in these late transition metals. Mingos discussed the electronic structure of the hypothetical $[Pt(PH_3)_2]_4$ clusters, in which terminal $PH_3$ bonding was assumed, and predicted counts of 56 or 54 electrons depending on the orientation of the ligands.[27]

Both the stability and diamagnetism of the title cluster are borne out in the molecular orbital (MO) diagram (Figure S2). There are 40 electrons that occupy all orbitals of the d manifold, forming a band of MOs centered on the edges and faces of the $Pd_4$ core. Overlap between symmetry-adapted ($4a_1$ + 2e) ligand group donor orbitals with combinations of metal-based $\sigma$-type 5s/5p cluster acceptor orbitals of matching symmetry leads to the formation of bonding MOs, lying energetically below the d block. These orbitals accommodate the eight donor electron pairs and account for metal−ligand bonding. A considerable gap of ∼2 eV separates the LUMO ($e_1$ symmetry) from the HOMO.

An energy decomposition analysis (EDA)[28,29] was carried out in order to compare the donor−acceptor capabilities of the terminal and face-capping stibine ligands and their interactions with the remaining $\{Pd_4(SbMe_3)_7\}$ fragment (Table 1). The

**Table 1. EDA Results of Cluster $[Pd_4(\mu_3\text{-}SbMe_3)_4(SbMe_3)_4]$[a]**

| | terminal | face-capping |
|---|---|---|
| $\Delta E_{Pauli}$ | +133.9 | +208.9 |
| $\Delta E_{elstat}$[b] | −118.4 (75.8%) | −161.7 (71.2%) |
| $\Delta E_{steric}$[c] | +15.5 | +47.2 |
| $\Delta E_{orb}$[b] | −37.8 (24.2%) | −65.5 (28.8%) |
| $\Delta E(A_1)$[d] | −21.8 (57.7%) | −32.9 (50.2%) |
| $\Delta E(A_2)$[d] | −0.3 (0.8%) | −0.8 (1.2%) |
| $\Delta E(E_1)$[d] | −15.7 (41.5%) | −31.7 (48.4%) |
| $\Delta E_{int}$ | −22.3 | −18.3 |
| $\Delta E_{prep}$ | +5.1 | +8.0 |
| $-D_e$ | −17.2 | −10.3 |
| $-D_e$ + dispersion | −43.8 | −53.6 |

[a]All energy values in kcal mol$^{-1}$. [b]Values in parentheses give percentage contributions to the total attractive interactions ($\Delta E_{elstat}$ + $\Delta E_{orb}$). [c]$\Delta E_{steric}$ = $\Delta E_{Pauli}$ + $\Delta E_{elstat}$ [d]Values in parentheses give percentage contributions to the total orbital interaction ($\Delta E_{orb}$). [e]$-D_e$ = $\Delta E_{int}$ + $\Delta E_{prep}$

terminal $SbMe_3$ ligand exhibits a larger fragment binding energy, $-D_e$, (−17.2 kcal mol$^{-1}$) compared to the face-capping motif (−10.3 kcal mol$^{-1}$). The face-capping location of the $\mu_3$-$SbMe_3$ ligand over a $\{Pd_3\}$ face results in enhanced interactions relative to the terminal $SbMe_3$ interacting with a single Pd center. Thus, $\mu_3$-$SbMe_3$ has a larger $\Delta E_{steric}$ (+47.2 vs +15.5 kcal mol$^{-1}$), but this is offset by a greater $\Delta E_{orb}$ (−65.5 vs −37.8 kcal mol$^{-1}$). The individual contributions to $\Delta E_{orb}$ are dominated by the $A_1$ and $E_1$ components equating to $\sigma$-donation (Sb → Pd) and $\pi$-back-donation (Sb ← Pd), respectively; both components are again more significant for the $\mu_3$-$SbMe_3$ ligand. It is striking that for both binding modes the electrostatic term $\Delta E_{elstat}$ makes a significantly larger contribution (71−76%) to the total metal−ligand bonding than the orbital term $\Delta E_{orb}$ (24−29%). A similar observation has been reported for terminal phosphines,[30] indicating that focusing on orbital interactions alone may be misleading.

Importantly, the ligand−cluster interactions are further stabilized by dispersion effects, yielding *total* fragment binding energies of −53.6 and −43.8 kcal mol$^{-1}$ for $\mu_3$-$SbMe_3$ and terminal $SbMe_3$, respectively, reversing the order of ligand binding relative to the electronic term alone.

The natural orbitals for chemical valence (NOCV)[31] scheme allows for further insight into the $\Delta E_{orb}$ term by highlighting the dominant deformation density channels. Isocontour plots of these channels aid visualization of $\sigma$-donation and $\pi$-back-donation in the cluster (Figure 4). For the terminal case, electron $\sigma$-donation from the Sb lone pair (5s) into the vacant



DOI: 10.1021/jacs.6b04060
J. Am. Chem. Soc. XXXX, XXX, XXX−XXX

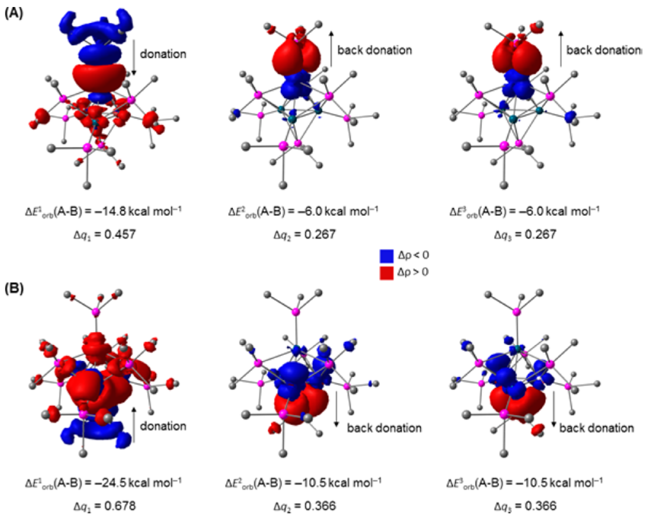


**Figure 4.** NOCV contour plots (isovalue 0.0005 au) of key deformation density channels describing the interaction between the cluster fragment $[Pd_4(SbMe_3)_7]$ and a $SbMe_3$ fragment in terminal (A) and face-capping (B) binding mode. Additionally, corresponding energy eigenvalues $\Delta E^k_{orb}$ and charges $\Delta q_k$ are shown. Electron flow is shown from blue to red.

Pd acceptor orbital (5s) makes a strong contribution to bonding ($\Delta E^1_{orb}$ = −14.8 kcal mol$^{-1}$). Two components of $\pi$-back-donation from Pd to Sb can also be clearly identified and are characterized by energies of $\Delta E^2_{orb} = \Delta E^3_{orb}$ = −6.0 kcal mol$^{-1}$. A similar analysis for the $\mu_3$-$SbMe_3$ fragment reveals an increase in the stabilization energies and associated charge flows for both the $\sigma$ ($\Delta E^1_{orb}$ = −24.5 kcal mol$^{-1}$) and $\pi$ channels ($\Delta E^2_{orb} = \Delta E^3_{orb}$ = −10.5 kcal mol$^{-1}$) due to the larger overlap area provided by the $Pd_3$ face, in line with the EDA analysis.

To summarize, a rare example of a halostibine complex with a transition metal halide has been synthesized and characterized as a dimer in the solid state, supported by secondary Sb···Cl interactions. This complex demonstrates unexpected reactivity with MeLi, resulting in isolation of a highly unusual $Pd(0)_4$ cluster with $\mu_3$-$SbMe_3$ ligands; the first example of triple bridging by a monodentate organopnictine. Computational modeling of the cluster reveals that both bridging and terminal $SbMe_3$ ligands can be efficient acceptors in metal-to-ligand $\pi$-back-donation, helping to stabilize the electron rich $\{Pd_4\}$ core. Investigation of potential phosphine and arsine analogues is underway in our group. The effect of this new pnictine bonding mode on the electronic environment of the transition metal could have considerable impacts in organometallic chemistry, including in the design of new homogeneous catalysts.

## ■ ASSOCIATED CONTENT

### Supporting Information

The Supporting Information is available free of charge on the ACS Publications website at DOI: 10.1021/jacs.6b04060.

Experimental and computational details (PDF)
Crystallographic data (CIF)
Crystallographic data (CIF)
Optimized coordinate file (XYZ)

## ■ AUTHOR INFORMATION

### Corresponding Authors

*sophie.benjamin@ntu.ac.uk
*t.kraemer@hw.ac.uk

### Notes

The authors declare no competing financial interest.

## ■ ACKNOWLEDGMENTS

The authors would like to thank the EPSRC for funding through grant reference EP/K039466/1. An allocation of computer time on the NSCCS is gratefully acknowledged.

## ■ REFERENCES

(1) Schwab, P.; Mahr, N.; Wolf, J.; Werner, H. *Angew. Chem., Int. Ed. Engl.* **1994**, *33*, 97.
(2) Werner, H. *Angew. Chem., Int. Ed.* **2004**, *43*, 938.
(3) Balch, A. L.; Davis, B. J.; Olmstead, M. M. *Inorg. Chem.* **1993**, *32*, 3937.
(4) Balch, A. L.; Davis, B. J.; Olmstead, M. M. *J. Am. Chem. Soc.* **1990**, *112*, 8592.
(5) Ke, I.; Gabbaï, F. P. *Aust. J. Chem.* **2013**, *66*, 1281.
(6) Schinzel, S.; Muller, R.; Riedel, S.; Werner, H.; Kaupp, M. *Chem. - Eur. J.* **2011**, *17*, 7228.
(7) Ke, I.; Jones, J. S.; Gabbaï, F. P. *Angew. Chem., Int. Ed.* **2014**, *53*, 2633.
(8) Wade, C. R.; Ke, I.; Gabbaï, F. P. *Angew. Chem., Int. Ed.* **2012**, *51*, 478.
(9) Benjamin, S. L.; Reid, G. *Coord. Chem. Rev.* **2015**, *297–298*, 168.
(10) Benjamin, S. L.; Levason, W.; Reid, G.; Warr, R. P. *Organometallics* **2012**, *31*, 1025.
(11) Braunschweig, H.; Dewhurst, R. D.; Hupp, F.; Wolf, J. *Chem. - Eur. J.* **2015**, *21*, 1860.
(12) Tschersich, C.; Limberg, C.; Roggan, S.; Herwig, C.; Ernsting, N.; Kovalenko, S.; Mebs, S. *Angew. Chem., Int. Ed.* **2012**, *51*, 4989.
(13) Lin, T.; Ke, I.; Gabbaï, F. P. *Angew. Chem., Int. Ed.* **2012**, *51*, 4985.
(14) Ke, I.; Gabbaï, F. P. *Inorg. Chem.* **2013**, *52*, 7145.
(15) Samochocka, K.; Fokt, I.; Anulewicz-Ostrowska, R.; Przewloka, T.; Mazurek, A. P.; Fuks, L.; Lewandowski, W.; Kozerski, L.; Bocian, W.; Bednarek, E.; Lewandowska, H.; Sitkowski, J.; Priebe, W. *Dalton Trans.* **2003**, 2177.
(16) Alvarez, S. *Dalton Trans.* **2013**, *42*, 8617.
(17) Benjamin, S. L.; Levason, W.; Light, M. E.; Reid, G.; Rogers, S. M. *Organometallics* **2014**, *33*, 2693.
(18) Brown, M. D.; Levason, W.; Reid, G.; Webster, M. *Dalton Trans.* **2006**, 5648.
(19) Burrows, A. D.; Mingos, D. M. P.; Menzer, S.; Vilar, R.; Williams, D. J. *J. Chem. Soc., Dalton Trans.* **1995**, 2107.
(20) Dubrawski, J.; Kriege-Simondsen, J.; Feltham, R. D. *J. Am. Chem. Soc.* **1980**, *102*, 2089.
(21) Molon, M.; Dilchert, K.; Gemel, C.; Seidel, R.; Schaumann, J.; Fischer, R. A. *Inorg. Chem.* **2013**, *52*, 14275.
(22) Bennett, M. J.; Cotton, F. A.; Winquist, B. H. *J. Am. Chem. Soc.* **1967**, *89*, 5366.
(23) Mednikov, E. G.; Eremenko, N. K.; Gubin, S. P.; Slovokhotov, Y. L.; Struchkov, Y. T. *J. Organomet. Chem.* **1982**, *239*, 401.
(24) Feltham, R. D.; Elbaze, G.; Ortega, R.; Eck, C.; Dubrawski, J. *Inorg. Chem.* **1985**, *24*, 1503.
(25) Burrows, A. D.; Machell, J. C.; Mingos, D. M. P. *J. Chem. Soc., Dalton Trans.* **1992**, 1991.
(26) Frost, P. W.; Howard, J. A. K.; Spencer, J. L.; Turner, D. G. *J. Chem. Soc., Chem. Commun.* **1981**, 1104.
(27) Evans, D.; Mingos, D. M. P *J. Organomet. Chem.* **1982**, *240*, 321.
(28) Morokuma, K. *J. Chem. Phys.* **1971**, *55*, 1236.
(29) Ziegler, T.; Rauk, A. *Theor. Chim. Acta.* **1977**, *46*, 1.
(30) Frenking, G.; Wichmann, K.; Fröhlich, N.; Loschen, C.; Lein, M.; Frunzke, J.; Rayón, V. M. *Coord. Chem. Rev.* **2003**, *238*, 55.
(31) Mitoraj, M. P.; Michalak, A.; Ziegler, T. *J. Chem. Theory Comput.* **2009**, *5*, 962.